Flue gas injection into gas hydrate reservoirs for methane recovery and carbon dioxide sequestration

Flue Gas Injection into Gas Hydrate Reservoirs for Methane Recovery and Carbon Dioxide Sequestration

Jinhai Yang[a*], Anthony Okwananke[a], Bahman Tohidi[a], Evgeny Chuvilin[b], Kirill Maerle[b], Vladimir Istomin[b], Boris Bukhanov[b], Alexey Cheremisin[b]

[a] Institute of Petroleum Engineering, School of Energy, Geoscience, Infrastructure and Society, Heriot-Watt University, Edinburgh EH14 4AS, United Kingdom

[b] Skolkovo Institute of Science and Technology, Mosco 143026, Russia

Abstract

Flue gas injection into methane hydrate-bearing sediments was experimentally investigated to explore the potential both for methane recovery from gas hydrate reservoirs and for direct capture and sequestration of carbon dioxide from flue gas as carbon dioxide hydrate. A simulated flue gas from coal-fired power plants composed of 14.6 mole% carbon dioxide and 85.4 mole% nitrogen was injected into a silica sand pack containing different saturations of methane hydrate. The experiments were conducted at typical gas hydrate reservoir conditions from 273.3 to 284.2 K and from 4.2 to 13.8 MPa. Results of the experiments show that injection of the flue gas leads to significant dissociation of the methane hydrate by shifting the methane hydrate stability zone, resulting in around 50 mole% methane in the vapour phase at the experimental conditions. Further depressurisation of the system to pressures well above the methane hydrate dissociation pressure generated methane-rich gas mixtures with up to 80 mole% methane. Meanwhile, carbon dioxide hydrate and carbon dioxide -mixed hydrates were formed while the methane hydrate was dissociating. Up to 70% of the carbon dioxide in the flue gas was converted into hydrates and retained in the silica sand pack.

* Corresponding author, email: jinhai.yang@hw.ac.uk

Keywords: Hydrate; Methane; Carbon dioxide; Flue gas; Methane recovery; Carbon dioxide sequestration

1 Introduction

An abundance of methane (CH_4) is trapped in gas hydrates in subsea sediments [1] and permafrost regions [2], although the actual volumes of gas hydrate deposits worldwide are still arguable [3]. Gas hydrates, a type of ice-like clathrate compounds, can be decomposed if the temperature and pressure are outside their hydrate stability zone (HSZ), or the chemical equilibrium between the hydrate phase and the adjacent environment is disturbed [4]. Based on this principle, several methods were suggested for methane recovery from gas hydrates in sediments, such as depressurisation, thermal stimulation, inhibitor injection [5], and carbon dioxide (CO_2) replacement [6], or combinations of the above.

Thermal stimulation brings heat into gas hydrate deposit layers by a variety of methods such as hot brine injection, steam injection, in-situ combustion, and electromagnetic heating. Laboratory experimental results showed that about 50% of the recovered energy would be consumed to generate the required heat for heating up the gas hydrate-bearing sediment [7]. Reservoir simulation indicated that thermal stimulation appears ineffective because of huge quantity of heat loss to porous media in the hydrate layer or the geologic formations in the vicinity [8], particularly for disperse low-saturation of gas hydrate deposits [9]. The Mallik 2002 gas hydrate research well programme tested the thermal stimulation technique at in situ conditions (907-920 m below surface, 8 °C and 10 MPa) [10]. It was found that, unless the hydrate layers exhibit sufficient thickness, hydrate saturation, and permeability, it is not economically viable to heat a large mass of a hydrate-containing formation by the thermal stimulation alone [11].

Inhibitor injection shifts the gas hydrate deposit conditions out of the hydrate stability zone (HSZ) by injecting alcohol such as methanol, monoethylene glycol, and diethylene glycol. A very large volume of methanol will be needed to treat the water in the hydrate layers and to deal with the dilution by the water from hydrate dissociation as well. Moreover, injected inhibitors could pose serious risk to damage the environment for the marine ecosystem. As a result, it is believed that inhibitor injection technique on its own will not be viable for any type of gas hydrate deposits [8].

Depressurisation method moves the hydrate reservoir conditions outside the HSZ by reducing the pressure in the gas hydrate reservoir. By comparison to the thermal stimulation technique and the inhibitor injection technique, it does not need to input additional energy or chemicals into the hydrate reservoir, therefore, is technically simple, effective, and prompt inducement to gas hydrate decomposition [12]. The depressurisation technique was successfully applied to produce methane from gas hydrate reservoirs in both onshore and offshore field tests. Messoyakha gas field in the West Siberian basin (Russia) is the only commercial production reservoirs of gas hydrates in the world, where natural gas has been produced from gas hydrate deposits since 1970s [13]. A series of scientific and engineering field trials were conducted in the Mackenzie Delta of Canadian Arctic. The Mallik 2002 gas hydrate production research well programme investigated the feasibility of gas hydrate production by thermal stimulation and depressurisation in short-term production experiments [14], while the results of the Mallik 2007/2008 programme demonstrated that natural gas can be produced from gas hydrate reservoirs by depressurisation alone [15]. Depressurisation method was also tested in the world first offshore methane recovery field trial in Nankai Trough, Japan [16]. All these hydrate sites are sandstone or marine sand reservoirs with high porosity, high permeability, and high hydrate saturation. However, Boswell and Collett estimated that such sandstone-bedded gas hydrates are only a small fraction of the total gas hydrate resources worldwide [17]. For the

overwhelming majority in low-permeability sediments or disperse distribution [18] of gas hydrates, depressurisation becomes ineffective. Additionally, for the hydrate reservoirs well inside the HSZ, the reservoir pressure has to be reduced very low to be able to dissociate the gas hydrates. As a consequence, depressurisation results in huge volume of water production, sediment instability, and sand production challenges [8]. Yamamoto et al. reported that sand produced during depressurisation blocked the downhole production device and terminated the gas production of the world's first offshore trial of gas production from marine hydrate reservoirs after six days of gas flow in the Eastern Nankai Trough, Japan [19].

CO_2 replacement method is based on the fact that chemical potential of methane hydrate is higher than that of CO_2 hydrate [20]. Theoretically, CO_2 molecules have relatively high tendency to replace the methane molecules from the methane hydrate cages, which was initially proposed by Ohgaki et al. [6]. Under ideal conditions such as high specific surface areas, high permeability, good heat and mass transfer the process of CO_2 displacement process could be fast and efficient. For example, nearly all methane in methane hydrate was replaced by CO_2 in two half cylindrical sandstone cores separated with a purpose-made spacer [21]. Shin et al. found that methane-isopentane hydrates almost completely disappeared after CO_2 replacement using high-power decoupling ^{13}C NMR and Raman spectra, in a mechanically stirred reactor [22]. It was also observed that CO_2 replacement occurred quickly in fine hydrate particles that were converted from ice powers in contact with methane [23]. In practice, for example, in sediments or in-situ hydrate reservoirs, the process is constrained by a number of geologic factors such as permeability, porosity, heat and mass transfer, and secondary hydrate formation. Experimental study showed that the presence of excess water and clays resulted in slow CO_2-CH_4 exchange rate [24]. It was also reported that high saturation of gas hydrates could lead to lower percentage of CO_2 replacement [25]. The undesired CO_2 hydrate or CO_2-CH_4 mixed hydrate could clog the pores in the sediments or isolate the methane hydrate from CO_2 by

forming CO_2 hydrate shells that coat on the methane hydrate crystals [26]. Recent results showed that the efficiency of CO_2 replacement technique could be improved by introduction of other gases. Masuda et al. experimentally investigated injection of a mixture of 60 mo% CO_2 and 40 mol% nitrogen (N_2) to improve the CO_2-CH_4 exchange rate and found that CO_2-CH_4 exchange ratios were about 30% for low hydrate-saturation and only 5% for high hydrate-saturation in the sand cores [27]. The experimental results from Kang et al. showed that injection of a simulated flue gas with 20 mol% CO_2 and 80 mol% N_2 increased the methane recovery ratio from 64 to 85% [28]. Kang et al. experimentally demonstrated that injection of CO_2 with air together can enhance CO_2-replacement process by decomposition-driven guest exchange mechanism [29]. Lee et al. reported the latest results showing that flue gas can be used to replace methane from structure H hydrates that was formed with methane and neohexane [30]. The first field trial of the CO_2 replacement technique was successfully conducted in the North Slope of Alaska [31]. 77% N_2 was added to the CO_2 stream to prevent secondary hydrate formation and have a high CO_2-CH_4 exchange rate [32]. Garapati,et al. conducted reservoir simulation to demonstrate how addition of N2 affect the dynamic process of gas production after injection of the CO_2-N_2 mixture [33]. In about 6 weeks of gas production, in total, 23.2 mscm (million standard cubic meters) CH_4 was produced at the well head; about 54% of the injected CO_2 was stored underground; and more than 50% of the produced methane was retained in the well until the well was further depressurised to below the methane hydrate dissociation pressure [34].

All the techniques reviewed above face challenges to be able to produce methane at an economically viable rate, although they appear technically feasible [35]. Development of novel techniques has therefore become crucial for the commercial viability of methane recovery from gas hydrate reservoirs. This work proposes direct injection of flue gas into gas hydrate reservoirs to decompose methane hydrates and recover methane from gas hydrates and

simultaneously sequester the CO_2 component of the flue gas as CO_2 hydrate or CO_2 mixed hydrates in the hydrate reservoir formations. Application of the flue gas injection method could substantially enhance the feasibility of depressurisation method for severe hydrate reservoir conditions and avoid CO_2 capture burden of geologic storage of CO_2.

2 Methods

The major constituents of flue gas are nitrogen and CO_2. For example, coal-fired flue gas (post-combustion) typically contains about 12-15% CO_2 and about 80% N_2 apart from water vapour and oxygen [36]. As a concept-proof work, for simplicity, deionised water and a simulated flue gas composed of 14.6 mol% CO_2 and 85.4 mol% N_2 were used. Injection of flue gas will move the thermodynamic conditions of the gas hydrate reservoir toward lower temperature and higher pressure. Figure 1 illustrates the HSZs of CO_2, methane, the simulated flue gas in the presence of water, which was predicted using our in-house thermodynamic model HydraFLASH [37]. It can be seen that 50 mol% of the flue gas can shift the methane hydrate phase boundary to the left by 3.5 K.

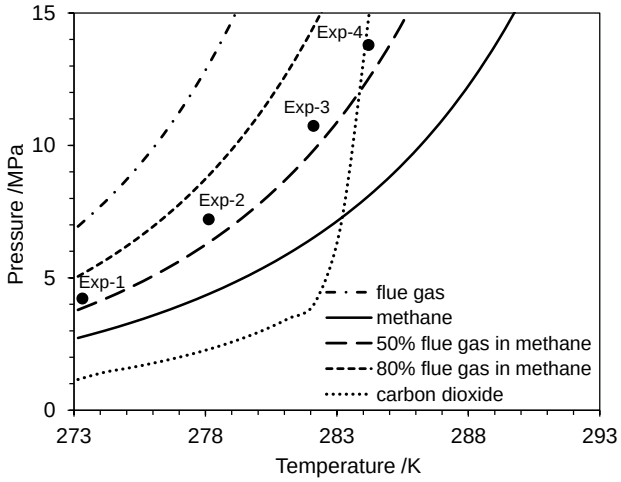

Figure 1 Predicted shifts in methane hydrate stability zone due to injection of flue gas and the experiment conditions

Depending on the composition and concentration of the injected flue gas, injection of the flue gas may result in shifting the hydrate reservoir conditions outside the methane HSZ hence dissociation of the methane hydrate. Methane hydrate decomposes into water and methane gas and the released methane gas will be mixed with the flue gas injected. The methane gas ratio in the gas mixture will gradually increase as more methane is released from hydrate dissociation. The hydrate decomposition will continue (though controlled by heat and mass transfer) until the HSZ back to a region where the temperature and pressure conditions in the hydrate-bearing sediments are located in the new HSZ of the mixed gas. In addition to the immediate decomposition due to the HSZ shift, the methane molecules originally trapped in the crystalline cages of the remaining methane hydrate could also be replaced by the CO_2 molecules in the injected flue gas, given that the tendency/driving force of CO_2-N_2 replacement is much weaker than CO_2 only. Anderson predicted the enthalpy of dissociation and hydration number of carbon dioxide hydrate and from the Clapeyron equation. His results showed that CO_2 replacement is a relatively weak exothermic reaction [38] although methane hydrate dissociation is also endothermic [39]. The overall consequence of the hydrate dissociation and CO_2 replacement will cause a reduction in the local temperature, which hinders the methane hydrate decomposition. Therefore, heat transfer also play an important role in methane recovery by flue gas injection.

Meanwhile, some of the CO_2 presents in the injected flue gas could be stored in the sediments through a variety of reactions. The CO_2 molecules could be combined with water in the pores and form CO_2 hydrate, CO_2 mixed hydrates such as CO_2-CH_4 and N_2-CO_2-CH_4, given that the typical gas hydrate reservoir conditions and limited CO_2 content of the flue gas do not favour the formation of CO_2-N_2 hydrate, N_2-CH_4 hydrate, and N_2 hydrate. CO_2-CH_4 molecule exchange may also occur and trap some CO_2 in a form of CO_2-CH_4 hydrate. Additionally, the CO_2 in the flue gas may also dissolve in the surrounding water at a typical solubility several

times higher than that of methane at similar temperature and pressure conditions, depending on the thermodynamic conditions and salinity. However, the amount of CO_2 dissolution in water is constrained by CO_2 partial pressure. Finally, the dissolved CO_2 could be converted into other solid minerals through mineralization reactions over geological time scale [40].

3 Experimental

Figure 2 shows the schematic diagram of the test set-up. The set-up comprises of a stainless steel cylindrical cell with a movable piston. The cell is 75 mm in diameter and 300 mm in length. Its effective volume is 800 cm^3. The piston is used to change the cell volume and to achieve the desired overburden pressure by applying hydraulic pressure behind the piston. A linear variable differential transmitter (LVDT) is mounted on the piston rod to determine the piston position hence the cell volume. A cooling jacket surrounding the cell is connected to a thermostat to achieve the required temperature. The set-up is equipped with a hand pump to initially adjust the overburden pressure and a Quizix pump to maintain the system pressure. The working temperature range of the set-up normally is 253 K to 323 K, and working pressure is up to 40 MPa. The system temperature is measured using a platinum resistance thermometer (PRT) (accuracy 0.1 K) and the system pressure and the overburden pressure are measured using two Druck pressure transducers (accuracy 0.05 MPa). A personal computer (PC) is used to record the system pressures, temperature, and the piston movement through a data acquisition device (DAD).

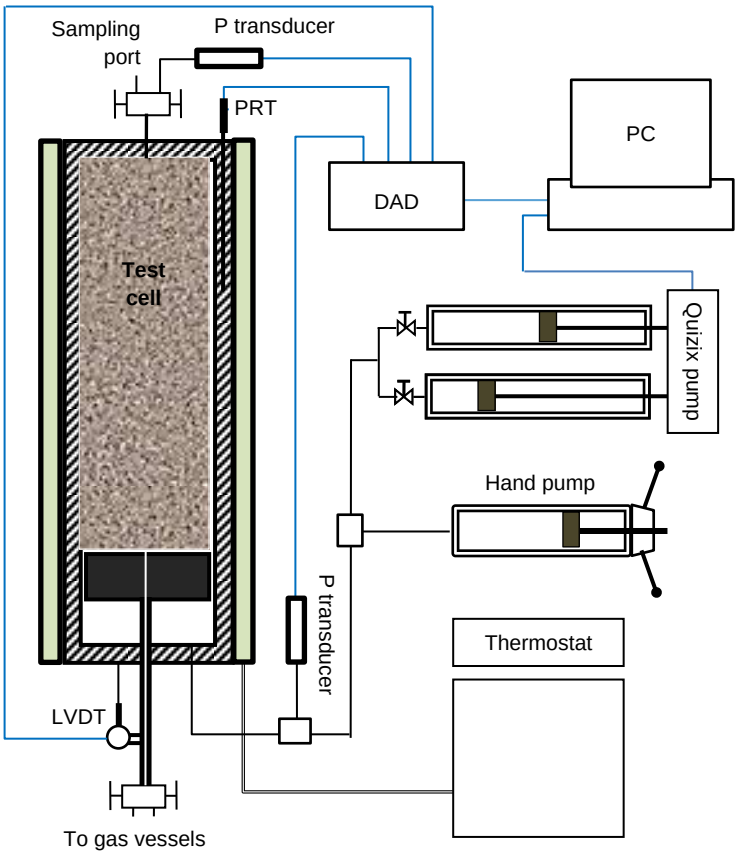

Figure 2 Schematic of the test set-up

The methane recovery tests were conducted in two steps, i.e., hydrate formation and methane recovery. In the first step, silica sand with a mass-medium size 256.5 µm was partially saturated with deionised water and then loaded into the test cell. After applying vacuum to remove air, an overburden pressure of 3.5 MPa was applied to compact the water-wetted sediment. Methane was injected in the compacted sediment until the desired pressure and the cell was cooled to just above the freezing temperature of water to form methane hydrate. Next, after completion of methane hydrate formation, synthetic flue gas was injected to purge the remaining methane gas. To minimise methane hydrate dissociation, the purging pressure was about 0.7 MPa higher than the dissociation pressure of the flue gas hydrate. After purging, the cell pressure was quickly reduced to the desired point by returning the piston, which expanded

the cell volume thus reduced the system pressure without any need for withdrawing any fluids from the test cell. Methane recovery process started once the desired pressure was reached. The system temperature and pressure were maintained constant until depressurisation stage started. The methane recovery process was monitored by taking a series of gas samples at pre-determined time intervals, while the system pressure was maintained by a dual-cylinder pump (Quizix SP-5200, Chandler Engineering). The gas samples were analysed using a gas chromatograph (Varian 3600, Agilent Technologies). The average calibration errors of the gas chromatograph were ±1.5% for methane, ±0.5% for carbon dioxide, and ±1.2% for nitrogen.

4 Experimental Results

This work was set to experimentally investigate the feasibility of the flue gas injection approach, i.e., to understand three fundamental issues: how methane hydrate decomposes after exposing to a methane-flue gas mixture, how flue gas affects depressurisation process, and whether or not the CO_2 in flue gas could be sequestered while methane hydrate is decomposing due to the presence of the flue gas. To understand these issues, the experiments were conducted at different temperature-pressure conditions. As shown in Figure 1, Experiments 1 to 3 were set inside both methane and CO_2 HSZs, while Experiment 4 was set outside CO_2 HSZ but inside methane HSZ. The experimental temperature covered the typical temperature conditions of naturally-occurring hydrate reservoirs from around 273.3 to 284.2 K, whilst the experiment pressures were set to allow the system to reach a new thermodynamic equilibrium with about 50 mol% methane in the vapor phase after flue gas injection.

Table 1 Methane recovery experiment conditions

Experiment	T (K)	P (MPa)	ϕ (%)	S_h (vol%)	S_g (vol%)	S_w (vol%)
1	273.3	4.2	39.0	60.2	28.3	11.5
2	278.1	7.2	37.7	54.4	26.0	19.6
3	282.1	10.7	37.7	48.8	27.1	24.0
4	284.2	13.8	37.0	47.3	25.5	27.2

Silica sand was used to simulate marine sediments. The sand was mixed with water to have around 55 pore volume% of water saturation. After vacuuming and compacting, methane was injected to pressurise the system to around 20 MPa at a room temperature of around 293 K. Methane hydrate was then formed by cooling the system directly to 273.3 K. After methane hydrate formation, the system was heated to the desired temperature and depressurised to the desired pressure. Finally, the saturation of methane hydrate, remaining water, and remaining methane gas was determined based on PVT calculations. Table 1 shows the experimental conditions before flue gas was introduced into the sand pack containing methane hydrate, including experimental temperature (T) and pressure (P), porosity (ϕ), methane hydrate saturation (S_h), remaining methane gas saturation (S_g), and remaining water saturation (S_w).

4.1 Decomposition kinetics at constant pressure

Methane recovery immediately started once the system was depressurised to the desired point after purging out most of the remaining methane gas. As a typical example, in Experiment 1, Figure 3 illustrates the kinetic process of methane decomposition after the flue gas was injected. In the first few hours from A to B, the methane hydrate is dissociated very fast, leading to a sudden increase in methane concentration from the initial value to above 40 mol% in the vapour phase. This is called quick dissociation stage (Stage 1). Masuda el al. showed very similar dissociation process for nitrogen-induced methane hydrate dissociation using their hydrate reservoir simulator [41]. The fast dissociation stage was also experimentally observed for air-induced hydrate dissociation by Haneda et al. [42]. From B to C in Stage 2, the methane was kept slow dissociation over about 160 hours and the methane concentration became constant after about 270 hours. Finally, from C to D in Stage 3, the system was depressurised in steps at the same temperature and more methane was produced from methane hydrate decomposition, which will be discussed in Section 4.2.

Such kinetic characteristics was observed in all four experiments, as shown in Figure 4. In Stage 1, the injected flue gas diluted/reduced methane concentration around methane hydrate crystals, therefore, shifted the gas hydrate stability zone. The methane hydrate quickly dissociated and released more methane to the vapor phase. The increase of the methane concentration made the system to approach a new thermodynamic equilibrium. In Stage 2, the methane concentration gradually rose to such a level that the system became very close to equilibrium. As a result, the methane hydrate decomposition was quickly slowed down. In fact, in the following discussion, it will be seen that mixed hydrates (e.g., CO_2-CH_4) formation was also occurring, which reduced the increasing rate of the methane in the vapor. Table 2 presents the experimentally determined methane concentrations and release rates at the end of the methane decomposition Stages 1 and 2. Most of the methane was recovered very quickly in Stage 1. In Stage 1 the methane recovery rate was more than 100 times higher than in Stage 2.

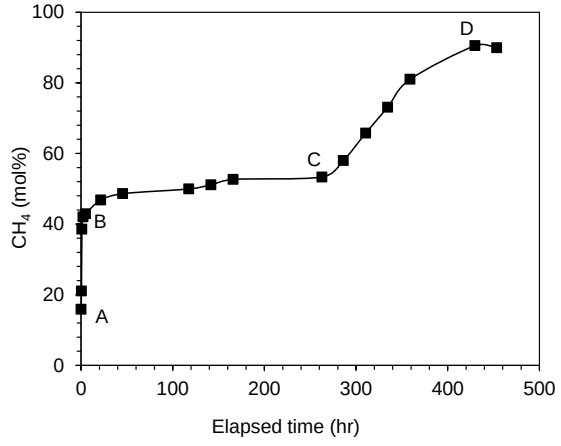

Figure 3 Methane recovery process was divided into three stages (Experiment 1)

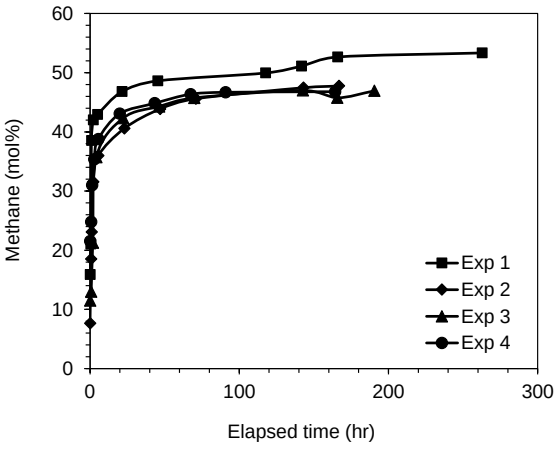

Figure 4 Changes in methane content after the flue gas was injected

Table 2 Determined methane concentration and CO_2 ratio in methane recovery by flue gas injection (Stages 1 and 2)

Experiment	T	P	Stage	CH_4 (mol%)			$CO_2/(CO_2+N_2)$ (%)	
	K	MPa		Initial	Final	Rate (mol/hr)	Initial	Final
1	273.3	4.2	1	15.9	42.9	0.0544	8.8	9.6
			2	42.9	53.3	0.00018	9.6	4.3
2	278.1	7.2	1	7.6	36.0	0.0565	11.4	14.6
			2	36.0	47.8	0.00049	14.6	6.0
3	282.1	10.7	1	11.5	35.7	0.0894	11.8	15.4
			2	35.7	46.9	0.00061	15.4	9.6
4	284.2	13.8	1	21.5	38.8	0.101	10.5	11.7
			2	38.8	46.7	0.00102	11.7	11.1

4.2 Depressurisation

Depressurisation was performed at a series of pressure steps after the new thermodynamic equilibrium was reached at the set pressure. The system was maintained at each pressure step over 24 hours to ensure equilibrium was achieved. Figure 5 illustrates how the methane was recovered during depressurisation. In Figure 5 the vertical dotted lines indicate the methane hydrate dissociation pressures at the corresponding experimental temperatures. The presence of the flue gas made it possible to produce methane from the methane hydrate by depressurisation well above the methane hydrate dissociation pressure. For example, depressurisation can produce the gas with more than 65 mol% methane at a pressure about 0.7 MPa above the methane hydrate dissociation pressure at 273.3 K (Experiment 1), with about 60 mol% methane at a pressure about 0.8 MPa above the methane hydrate dissociation pressure at 278.1 K (Experiment 2), and with 55 mol% methane at a pressure about 1.4 MPa above the methane hydrate dissociation pressure at 282.1 K (Experiment 3). In Experiment 4 the methane hydrate was almost fully decomposed before depressurisation so that no much more methane was released during depressurisation before the system pressure became lower than the methane hydrate dissociation pressure, i.e., 8.1 MPa at 284.2 K.

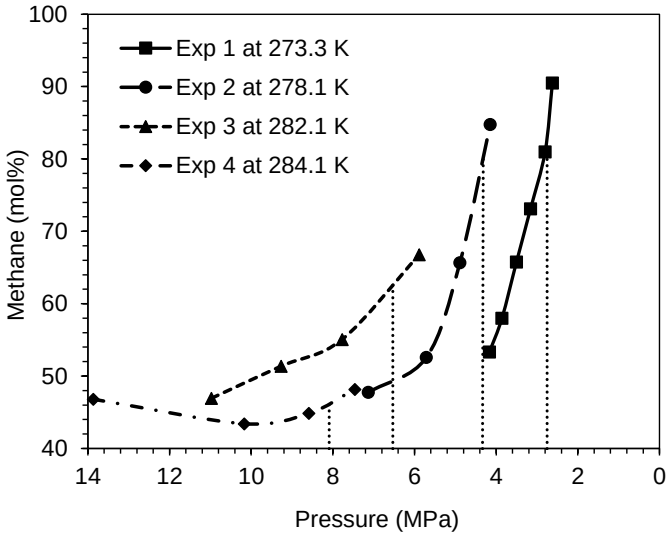

Figure 5 Methane hydrate starts decomposition well inside the methane HSZ

Injection of flue gas leads to methane hydrate decomposition at a pressure well above the methane hydrate dissociation pressure. This may make it possible to minimize the required depressurization degree of a hydrate reservoir to be able to produce methane gas from the hydrate. Minimized depressurization means limited pressure difference between the hydrate reservoir and the production well, hence less driving force for water flow and sand migration. Furthermore, the remaining reservoir pressure will also eliminate or reduce the requirement of external pumps to lift the produced water to allow the gas flow [8]. This could substantially improve the feasibility of the depressurization method for severe gas hydrate reservoir conditions such as low permeable Class 1 hydrate deposits with low permeability, Classes 2 and 3 that are deep inside the HSZ, and dispersive distributed hydrate deposits [12].

4.3 CO_2 sequestration

The potential of the flue gas injection method was also examined for CO_2 capture and storage in hydrate reservoirs. In Figure 6 the ratio of $CO_2/(CO_2 + N_2)$ is used as an indicator of the reduction of the absolute CO_2 content due to formation of CO_2 hydrate or CO_2-involved mixed hydrates, given that N_2-CH_4 and N_2-CO_2 hydrates cannot form at the experimental conditions

according to thermodynamic modelling. The concentrations of CO_2, nitrogen, and methane are also plotted in Figure 6 to enable analysis of the kinetic process of CO_2-involved hydrate formation.

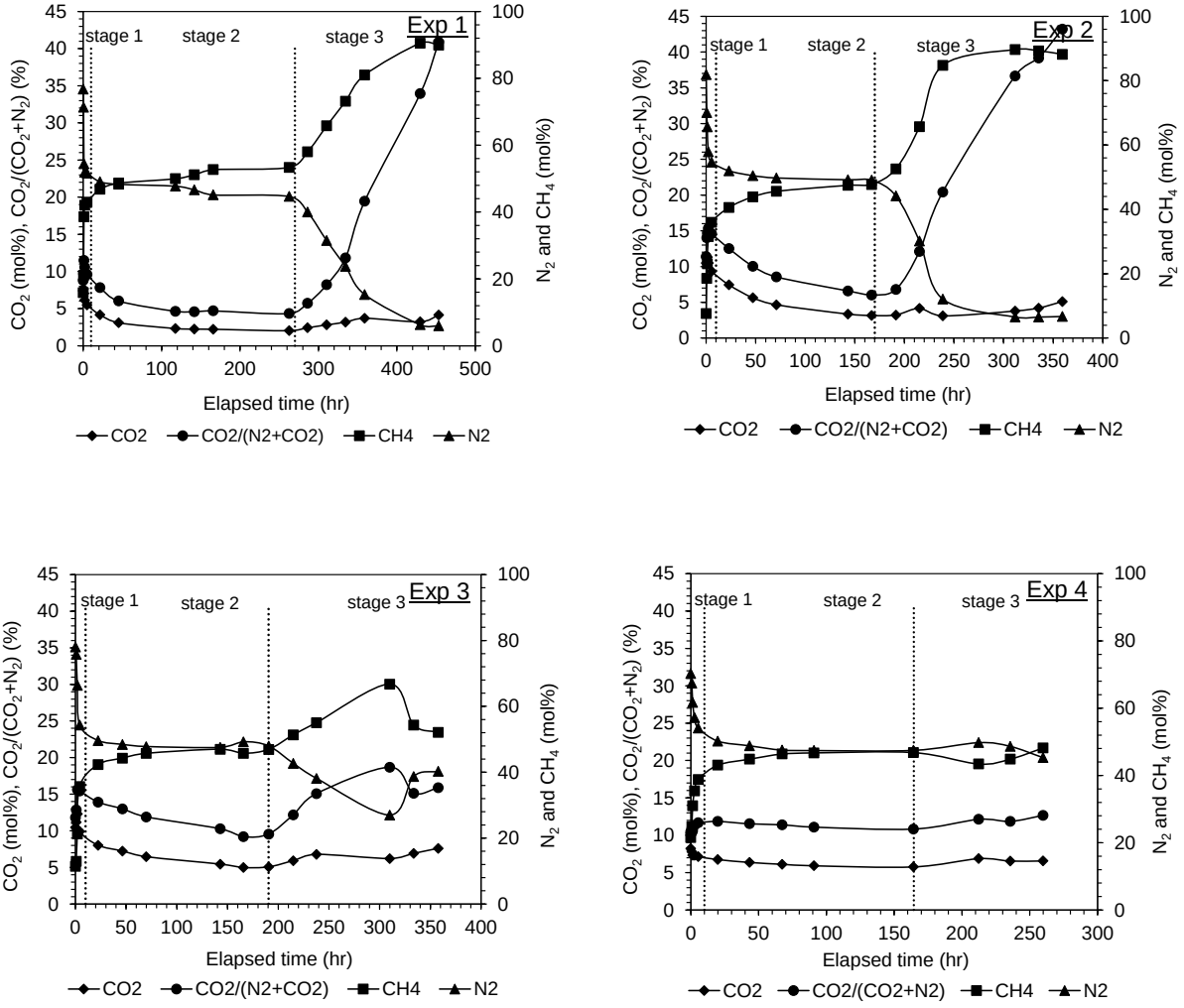

Figure 6 Changes in CO_2 content in vapour phase after flue gas injection and during depressurisation

In Stages 1 and 2, methane hydrate continuously dissociated as its phase equilibrium was broken by the injected flue gas, which leads to reduction in the concentration of CO_2 and nitrogen. Most importantly, the CO_2 ratio also continuously decreased. The reduction in the CO_2 ratio suggests that the CO_2 molecules in the vapour phase were converted into hydrates.

Thermodynamically, the CO_2 could be trapped in any types of a simple CO_2 hydrate, CO_2-CH_4 hydrate, and N_2-CO_2-CH_4 hydrate. The CO_2 content decreased to the minimum value at the end of Stage 2, where a new thermodynamic equilibrium was reached. In Experiments 1 to 3, the CO_2 ratio kept rising during depressurisation, indicating CO_2 was being released from decomposition of those mixed CO_2 hydrates. According to thermodynamic modelling, the N_2-CO_2-CH_4 hydrate was dissociated before the system was depressurised out of the methane HSZ, while the CO_2-CH_4 hydrate could not fully dissociate until the system was depressurised out of the CO_2 HSZ. However, the appearance of the maximum methane concentration implies that the methane hydrate and CO_2-CH_4 mixed hydrate were fully dissociated at the second last point at (273.3 K, 2.80 MPa) in Experiment 1, at the third last point (278.1 K, 2.99 MPa) in Experiment 2, at the third last point (281.1 K, 5.88 MPa) in Experiment 3, and at the fourth last point (284.2 K, 13.87 MPa) in Experiment 4. In Figure 6 more CO_2 was released from CO_2 hydrate at the last point at (273.3 K, 0.85 MPa) in the Experiment 1 plot, the last point at (278.1 K, 1.72 MPa) in the Experiment 2 plot, and the last point at (281.1 K, 3.79 MPa) in the Experiment 3 plot, where these points were outside the CO_2 HSZ. There was no such a rise in the CO_2 content observed, as Experiment 4 was conducted just outside the CO_2 HSZ, as shown in Figure 1.

Table 3 The amount of CO_2 in the vapour phase captured in hydrates*

Experiment	Temperature	CO_2 in vapour (mole)		CO_2 in hydrates	
	(K)	Initial	Final	(mole)	(%)
1	273.3	0.0358	0.0106	0.0252	70.4
2	278.1	0.0561	0.0177	0.0384	68.5
3	282.1	0.1369	0.0710	0.0659	48.1
4	284.2	0.1287	0.1096	0.0191	14.8

* CO_2 dissolution in water is small and negligible compared to inclusion in gas hydrates.

Table 3 shows the amount of CO_2 in the vapour phase captured in hydrates. The initial CO_2 content was measured in the vapour phase after completion of purging the remaining methane and the final CO_2 content was measured at the end of Stage 2 prior to depressurisation. 70.4%, 68.5%, 48.1%, and 14.8% of CO_2 initially in the vapour phase were captured and retained in the hydrates in the porous media in Experiments 1 to 4, respectively. This demonstrates two advantages over the conventional hydrate-based CO_2 capture (HBCC) method. A multi-stage HBCC process with 1 mol% tetra-n-butyl ammonium bromide has to be applied to achieve the CO_2 split fractions similar to those that was gained in Experiments 1 and 2 [43]. The CO_2 hydrate formation not only directly capture CO_2 from the flue gas and store it in the hydrate reservoir formation, but also could reduce the impact of methane hydrate decomposition on the wellbore and seafloor stability. Furthermore, the results suggest that deepness inside the CO_2 hydrate HSZ plays a substantial role in the CO_2 sequestration from the flue gas, given that the four experiments were conducted in a similar deepness inside the methane hydrate phase boundary (Figure 1). This is understandable because the conditions deeply inside the CO_2 HSZ would provide stronger driving force to promote formation of more CO_2 hydrate, CO_2-CH_4 hydrate, and N_2-CO_2-CH_4 hydrate. If taking into account the sharp slope change in CO_2 hydrate phase boundary at about 282 K, it would be generally suggest that the hydrate reservoirs at low temperatures could be better choices for CO_2 capture and storage by flue gas injection.

5 Discussions

Methane recovery by flue gas injection involves complex reactions. Figures 3 and 4 show that the methane hydrate quickly dissociated once the flue gas was introduced into the sand pack containing methane hydrate, methane gas, and water. In an in-situ hydrate reservoir the rate of the methane hydrate decomposition may be dominantly controlled by heat transfer in Stage 1 due to the fast heat absorption from the endothermic reaction of methane hydrate decomposition [41]. In Stage 2 the methane hydrate decomposed very slowly as the methane-

carbon dioxide-nitrogen mixture was approaching the new phase equilibrium with the remaining methane hydrate. Fresh flue gas-rich gas mixture is needed to continue dissociating the methane hydrate. The permeability of the porous media will be important for the mass transfer process. In other words, the methane recovery rate may be mainly constrained by mass transfer in Stage 2. Moreover, in addition to methane hydrate decomposition, the kinetics of the methane recovery by flue gas injection is rather more complex compared to conventional depressurisation, thermal stimulation, and CO_2-CH_4 replacement. Flue gas injection results in formation of various hydrates such as CO_2 hydrate, CO_2-CH_4 hydrate, N_2-CO_2-CH_4 hydrates, and possible CO_2 replacement as well. The existing kinetic models [44] need to be coupled with a thermodynamic model to be able to simulate the kinetic process of methane recovery by flue gas injection.

In Figure 6 it can be seen that the CO_2 ratio to the sum of CO_2 and nitrogen kept increasing till the system was depressurised out of the CO_2 HSZ. The ratio became much higher than its initial value. This is attributed to the fact that some of the CO_2 hydrate, N_2-CO_2-CH_4 hydrate, and N_2-CO_2 hydrate could be formed during the flue gas injection and the purge of the remaining methane, which was not measured in the first gas sample. Thermodynamically, the N_2-CO_2-CH_4 hydrate can stay as long as the system pressure is higher than the methane hydrate dissociation pressure, while the formed CO_2 hydrate and CO_2-CH_4 hydrate can stay as long as the system is not depressurised out of the CO_2 HSZ. This feature can enhance the security to retain CO_2 in the hydrate reservoir formation when methane is recovered.

The amplitude of the shift in the required depressurization pressure depends on the methane content in the produced gas. For example, in Experiment 2 at 278.1 K (Figure 5), about 66 mol% methane in the vapor phase needs to depressurize the system to 0.5 MPa above the methane hydrate dissociation pressure, 53 mol% and 48 mol% methane need 1.3 MPa and 2.7 MPa above the methane hydrate dissociation pressure, respectively. Methane is recovered in a

CH_4-N_2-CO_2 mixture. Therefore, gas separation is required to separate the methane from the produced methane-rich gas mixtures containing nitrogen and residual CO_2, which might constrict the cost effectiveness of the flue gas injection method to some extent. Fortunately, there are some gas separation technologies that have been used to separate methane from the CH_4-N_2 and CH_4-N_2-CO_2 gas mixtures for the enhanced coalbed methane recovery (ECBM) [45]. It was found that polyimide membranes could be used to separate N_2 or CO_2 from natural gases [46]. White et al. indicated that removal of N_2 from ECBM gas mixtures is economically feasible for N_2 content up to 30% [47].

6 Conclusions

Flue gas injection into gas hydrate-bearing sediments was experimentally investigated for methane recovery and CO_2 sequestration. The results show that injection of the flue gas results in fast dissociation of the methane hydrate by shifting the methane hydrate stability zone. The methane concentration in the vapour phase reached over 50 mol% at the typical methane hydrate reservoir conditions from 273.3 K and 4.2 MPa to 284.2 K and 13.8 MPa. Further depressurisation of the system to pressures well above the methane hydrate dissociation pressure produced methane in methane-rich gas mixtures and the methane concentration could be up to 80 mol%, depending on the experimental temperature and pressure. It was also found that CO_2 hydrate and some CO_2 mixed hydrates such as N_2-CO_2-CH_4 hydrate and CO_2-CH_4 hydrate were formed during the methane recovery after the flue gas was injected. About 70% of the CO_2 in the flue gas was converted into hydrates and retained in the silica sand pack. As a result, the flue gas injection method has considerable potentials to improve the economic viability and feasibility of methane recovery from gas hydrate reservoirs and CO_2 capture and storage in geological formations.

Acknowledgments

This work was financially supported by the Skolkovo Institute of Science and Technology, Russia, which is acknowledged gratefully.

References

[1] Kvenvolden K.A. 1988. Methane hydrates—a major reservoir of carbon in the shallow geosphere? *Chemical Geology*, **71,** 41-51.

[2] Collett T.S. 19921. Potential of gas hydrates outlined. *Oil & Gas Journal*, **90** (22), 84-87.

[3] Milkov A. V. 2004. Global estimates of hydrate-bound gas in marine sediments: how much is really out there? *Earth-Science Reviews,* **66,** 183-197

[4] Sloan E. D. Jr. 1998. *Clathrate Hydrates of Natural Gases*. Marcel Dekker Inc.: New York.

[5] Holder G. D., Kamath V. A., Godbole S. P. 1984. The potential of natural gas hydrates as an energy resource. *Annual Review of Energy,* **9,** 427-445.

[6] Ohgaki K., Takano K., Sangawa H., Matsubara T., Nakano S. 1996. Methane exploitation by carbon dioxide from gas hydrates- Phase Equilibria for CO_2-CH_4 mixed hydrate system. *Journal of Chemical Engineering of Japan*, **29**, 478-483.

[7] Tang L.G., Xiao R., Huang C., Feng Z.P., Fan S.S. 2005. Experimental investigation of production behaviour of gas hydrate under thermal stimulation in unconsolidated sediment. *Energy & Fuels*, **19**, 2402-2407.

[8] Moridis G.J., Collett T.S., Pooladi-Darvish M., Hancock S., Santamarina C., Boswell R., Kneafsey T., Rutqvist J., Kowalsky M.B., Reagan M.T., Sloan E.D., Sum A.K., Koh C.A. 2011. Challenges, uncertainties, and issues facing gas production from gas-hydrate deposits. SPE Reservoir Evaluation & Engineering, **14**, 76-112.

[9] Moridis G.J. and Sloan E.D. 2007. Gas production potential of disperse low-saturation hydrate accumulations in oceanic sediments. *Energy Conversion and Management*, **48**, 1834–1849.

[10] Dallimore S.R. and Collett T.S., eds. 2005. Scientific results from the Mallik 2002 gas hydrate production research well program, Mackenzie Delta, Northwest Territories, Canada: *Geological Survey of Canada Bulletin*, **585**.

[11] Collett T., Bahk J.J., Frye M., Goldberg D., Husebo J., Koh C., Malone M., Torres M. 2013. Historical methane hydrate project review. Report of project DE-FE0010195 prepared for the U.S. Department of Energy---National Energy Technology Laboratory.

[12] Moridis G.J. and Collett T.S. 2003. Strategies for gas production from hydrate accumulations under various geological and reservoir conditions. Proceedings of *TOUGH Symposium*, Lawrence Berkeley National laboratory, Berkeley, California, May 12-14, 2003.

[13] Makogon Y.F., Trebin F.A., Trofimuk A.A., Tsarev V.P., Cherskiy N.V. 1972. "Detection of a Pool of Natural Gas in a Solid (Hydrate Gas) State," *Doklady Academy of Sciences, USSR, Earth Science Section*, **196**, 197-200.

[14] Collett T.S. 2005. Results at Mallik highlight progress in gas hydrate energy resource research and development. *Petrophysics*, **46** (3), 237–243.

[15] Kurihara M., Sato A., Funatsu K., Ouchi H., Yamamoto K., Numasawa M., Ebinuma T., Narita H., Masuda Y., Dallimore S.R., Wright F., Ashford D. 2010. Analysis of production data for 2007-2008 Mallik gas hydrate production tests in Canada. SPE 132155, presented at *the CPS/SPE International Oil & Gas Conference and Exhibition* in China, Beijing, China, 8-10 June 2010.

[16] Fujii T., Suzuki K., Takayama T., Tamaki M., Komatsu Y., Konno Y., Yoneda J., Yamamoto K., Nagao J. 2015. Geological setting and characterization of a methane hydrate reservoir distributed at the first offshore production test site on the Daini-Atsumi Knoll in the eastern Nankai Trough, Japan. *Marine and Petroleum Geology*, **66**, 310-322.

[17] Boswell R. and Collett T. 2006. The gas hydrates resource pyramid, US DOE, *Fire in the Ice*, **6** (3), 5-7.

[18] Konno Y., Masuda Y., Akamine K., Naiki M., Nagao J. 2016. Sustainable gas production from methane hydrate reservoirs by the cyclic depressurization method. *Energy Conversion and Management*, **108**, 439–445.

[19] Yamamoto K., Terao Y., Fujii T., Ikawa T., Seki M. 2014. Operational overview of the first offshore production test of methane hydrates in the Eastern Nankai Trough. OTC 25243, presented at *the 2014 Offshore Technology Conference*, Houston, Texas, U.S.A., 5–8 May 2014.

[20] Seo Y.T. and Lee H. 2001. Multiple-phase hydrate equilibria of the ternary carbon dioxide, methane, water mixtures. *Journal of Physical Chemistry* B, 105 (41), 10084-10090.

[21] Erslanda G., Husebøa J., Grauea A., Baldwinb B.A., Howardc J., Stevens J. 2010. Measuring gas hydrate formation and exchange with CO_2 in Bentheim sandstone using MRI tomography. *Chemical Engineering Journal*, **158**, 25–31.

[22] Shin K., Park Y., Cha M., Park K.P., Huh D.G., Lee J., Kim S.J., Lee H. 2008. Swapping phenomena occurring in deep-sea gas hydrates. *Energy & Feuls*, **22**, 3160-3163.

[23] Lee B. R., Sloan E. D., Koh C. A., Sum A. K.. 2013. Energy production from gas hydrate system using CO_2 and CO_2/N_2 injection. SPE 168883 /URTecC 1614231, presented at *the Unconventional Resources Technology Conference*, Denver, Colorado, U.S.A., 12-14 August 2013.

[24] Yang J., Chapoy A., Tohidi B., Jadhawar P.S.; Lee J., Huh D.G. 2008. Thermodynamic conditions and kinetics of integrated methane recovery and carbon dioxide sequestration. OTC 19326, presented at *the 2008 Offshore Technology Conference*, Houston, Texas, U.S.A., 5–8 May 2008.

[25] Yuan Q., Sun C.Y., Liu B., Wang X., Ma Z.W., Ma Q.L., Yang L.Y., Chen G.J., Li Q.P., Li S., Zhang K. 2013. Methane recovery from natural gas hydrate in porous sediment using pressurised liquid CO_2. *Energy Conversion and Management*, **67**, 257-264.

[26] Parshall J. 2012. Production method for methane hydrate sees scientific success, *Journal of Petroleum Technology*, **64** (8), 50-51.

[27] Masuda Y., Maruta H., Naganawa S., Amikawa K. 2011. Methane recovery from hydrate-bearing sediments by N_2-CO_2 gas mixture injection: experimental investigation on CO_2-CH_4 exchange ratio. *Proceedings of the 7th International Conference on Gas Hydrates, Edinburgh, Scotland, United Kingdom, July 17-21, 2011*

[28] Kang H., Koh D.Y., Kim D., Park J., Cha M., Lee H. 2012. Recovery of methane intercalated in natural gas hydrate sediments using a carbon dioxide and flue gas mixture. *Proceedings of the Twenty-second (2012) International Offshore and Polar Engineering Conference, Rhodes, Greece, June 17–22, 2012.*

[29] Kang H., Koh D.Y., Lee H. 2014. Nondestructive natural gas hydrate recovery driven by air and carbon dioxide. *Scientific Reports*. 4:6616, DOI: 10.1038/srep06616.

[30] Lee Y.Seo Y.J., Ahn T., Lee J., Lee J.Y., Kim S.J., Seo Y., 2017. CH4 – Flue gas replacement occurring in sH hydrates and its significance for CH_4 recovery and CO_2 sequestration. *Chemical Engineering Journal*, **308**, 50–58.

[31] Schoderbek D. and Boswell R. 2011. Igńik Sikumi #1, Gas hydrate test well, successfully installed on the Alaska North Slope, *Fire in the Ice*, **11** (1), 1-5.

[32] Schoderbek D., Martin K. L., Howard J., Silpngarmlert S., Hester K. 2012. North slope hydrate fieldtrial: CO_2/CH_4 exchange. OTC 23725, presented at *the 2012 Offshore Technology Conference*, Houston, Texas, U.S.A., 3-5 December 2012.

[33] Garapati N., McGuire P., Anderson B. 2013. Modeling the injection of carbon dioxide and nitrogen into a methane hydrate reservoir and the subsequent production of methane gas on the North Slope of Alaska. SPE

168861 /URTecC 1583553, presented at *the Unconventional Resources Technology Conference*, Denver, Colorado, U.S.A., 12-14 August 2013.

[34] Schoderbek D., Martin K.L., Howard J., Silpngarmlet S., Hester K. 2012. North slope hydrate fieldtrial: CO_2/CH_4 exchange. OTC 23725, presented at *the Arctic Technology Conference*, Houston, Texas, U.S.A., 3-5 December 2-12.

[35] Walsh M.R., Hancock S.H., Wilson S.J., Patil S.L., Moridis G.J., Boswell R., Collett T.S., Koh C.A., Sloan E.D. 2009. Preliminary report on the commercial viability of gas production from natural gas hydrates. *Energy Economics*, **31**, 815–823.

[36] Metz B., Davidson O., de Coninck H.C., Loos M., Meyer L.A., Eds. 2005. *IPCC special report on carbon dioxide capture and storage*; Cambridge University Press: Cambridge, United Kingdom and New York, NY, USA.

[37] Haghighi H., Chapoy A., Burgess R., Tohidi B. 2009. Experimental and thermodynamic modelling of systems containing water and ethylene-glycol: application to flow assurance and gas processing. *Fluid Phase Equilibria*, **276**, 24-30.

[38] Anderson G.K. 2003. Enthalpy of dissociation and hydration number of carbon dioxide hydrate from the Clapeyron equation. *Journal of Chemistry Thermodynamics*, **35** (7), 1171-1183.

[39] Anderson G.K. 2004. Enthalpy of dissociation and hydration number of methane hydrate from the Clapeyron equation. *Journal of Chemistry Thermodynamics*, **36** (12), 1119-1127.

[40] Gunter W.D., Bachu S., Benson S.M. 2004. The role of hydrogeological and geochemical trapping in sedimentary basins for secure geological storage for carbon dioxide. In *Geological Storage of Carbon Dioxide*. Baines, S. J; Worden, R. H. Eds.; Geological Society: London, U.K., Special Publication, **233**, 129-145.

[41] Masuda Y., Konno Y., Hasegawa T., Haneda H., Ouchi H., Kurihara M. 2008. Prediction of methane hydrate dissociation behaviour by nitrogen gas injection. *Proceedings of the 6th International Conference on Gas Hydrates*, Vancouver, British Columbia, Canada, July 6-10, 2008.

[42] Haneda H., Sakamoto Y., Kawamura T., Aoki K., Komai T. 2005. Experimental study on dissociation behaviour of methane hydrate by air. *Proceedings of the 5th International Conference on Gas Hydrates*, Trondheim, Norway, June 12-16, 2005.

[43] Babu P., Linga P., Kumar R., Englezos P. 2015. A review of the hydrate based gas separation (HBGS) process for carbon dioxide pre-combustion capture. *Energy*, **85,** 261-279.

[44] Kim H.C., Bishnoi P.R., Heidemann R.A., Rizvi S.S.H. 1987. Kinetics of methane hydrate decomposition. *Chemical Engineering Science*, **42**, 2659-2666.

[45] Reeves S. and Oudinot A. 2005. The Tiffany Unit N2-ECBM pilot – A reservoir and economic analysis. Paper 0523, presented *the 2005 International Coalbed Methane Symposium*, Tuscaloosa, Alabama, USA, 18−19 May, 2005.

[46] Cecopieri-Gómez M.L., Palacios-Alquisira J., Domínguez J.M. 2007. On the limit of gas separation in CO_2/CH_4, N_2/CH_4 and CO_2/N_2 binary mixtures using polyimide membranes. *Journal of Membrane Science*, **293**, 53-65.

[47] White C.M., Smith D.H., Jones K.L., Goodman A.L., Jikich S.A., LaCount R.B., DuBose S.B., Ozdemir E., Morsi B.I., Schroeder K.T. 2005. Sequestration of carbon dioxide in coal with enhanced coalbed methane recovery – A review. *Energy & Fuels*, **19**, 659-724.